

Title	Formation Energies of Substitutional Sodium and Potassium in Hydroxyapatite
Author(s)	Matsunaga, Katsuyuki; Murata, Hidenobu
Citation	MATERIALS TRANSACTIONS (2009), 50(5): 1041-1045
Issue Date	2009-05
URL	<a href="http://hdl.handle.net/2433/109951">http://hdl.handle.net/2433/109951</a>
Right	Copyright (c) 2009 The Japan Institute of Metals
Type	Journal Article
Textversion	publisher

# Formation Energies of Substitutional Sodium and Potassium in Hydroxyapatite

Katsuyuki Matsunaga<sup>1,2</sup> and Hidenobu Murata<sup>1,\*</sup>

<sup>1</sup>Department of Materials Science and Engineering, Kyoto University, Kyoto 606-8501, Japan

<sup>2</sup>Nanostructures Research Laboratory, Japan Fine Ceramics Center, Nagoya 456-8587, Japan

First-principles calculations are performed to investigate atomic and electronic structures of Na<sup>+</sup> and K<sup>+</sup> ions substituting for Ca<sup>2+</sup> in hydroxyapatite (HAp). Formation energies of the substitutional defects are obtained from total energies of defective HAp supercells and chemical potentials determined by assuming chemical equilibrium between HAp and HAp-saturated aqueous solution containing Na<sup>+</sup> or K<sup>+</sup>. It is found that substitutional Na<sup>+</sup> with a charge-compensating interstitial proton is more stably formed, as compared to substitutional K<sup>+</sup>. This may be related to the fact that Na<sup>+</sup> is generally more abundantly involved in bones and tooth enamels than K<sup>+</sup>.

[doi:10.2320/matertrans.MC200819]

(Received November 4, 2008; Accepted December 15, 2008; Published February 12, 2009)

**Keywords:** hydroxyapatite, electronic structure calculation, ionic substitution, defect association, solution pH

## 1. Introduction

It is well known that an inorganic component of bone and tooth in human beings is hydroxyapatite (HAp, Ca<sub>10</sub>(PO<sub>4</sub>)<sub>6</sub>(OH)<sub>2</sub>) but contains various kinds of trace elements and point defects in its crystal lattice.<sup>1,2</sup> As trace elements, sodium (Na<sup>+</sup>) and magnesium (Mg<sup>2+</sup>) are main cationic impurities in HAp components of human enamels and bones (around 0.5–1.0 mass%), and a lesser amount of potassium (K<sup>+</sup>, 0.03–0.10 mass%) is also included. In contrast, the typical anionic impurities are 4–8 mass% of carbonate (CO<sub>3</sub><sup>2-</sup>) and ~ less than 0.3 mass% of fluoride (F<sup>-</sup>) and chloride (Cl<sup>-</sup>). Since these trace elements affect physical and chemical properties of biological HAp, it is important to understand a formation mechanism and thermodynamic stability of the impurity ions in HAp.

Among the trace elements involved in biological HAp, monovalent cations of Na<sup>+</sup> and K<sup>+</sup> are investigated in the present study. This is because Na<sup>+</sup> and K<sup>+</sup> impurities are expected to play important roles in bone mineralization, cell adhesion, and biochemical processes.<sup>3–5</sup> When atomic-level location of the monovalent impurities is considered, it is likely that the impurities substitute for Ca<sup>2+</sup> ions in the HAp lattice. The ionic radius of Na<sup>+</sup> (0.102 nm) is close to that of Ca<sup>2+</sup> (0.100 nm), while K<sup>+</sup> (0.138 nm) is much larger in size.<sup>6</sup> Such ionic-size differences will also influence stability of the substitutional impurities. Moreover, substitutions of Na<sup>+</sup> and K<sup>+</sup> at Ca<sup>2+</sup> sites of HAp result in charge imbalance, and thus formation of extra charge compensating defects is required so as to maintain charge neutrality of the system. In order to understand a defect formation mechanism of substitutional Na<sup>+</sup> and K<sup>+</sup>, electronic and atomic structures of the substitutional defects in HAp are calculated in a first-principles manner, and their formation energies and essential factors to determine their defect stability are investigated.

So far, a number of first-principles studies of point defects in HAp have been reported.<sup>7–14</sup> In particular, our research group recently proposed the thermodynamic treatment of first-principles total energies to analyze defect stability under chemical equilibrium between solid and aqueous solution.

The methodology was applied to intrinsic and extrinsic defects in calcium phosphates, and revealed the effect of solution pH on formation energies and concentrations of the defects.<sup>12–14</sup> Since the chemical equilibrium condition with aqueous solution is important to consider the point defect chemistry in HAp, the above methodology is also used in the present study to analyze thermodynamic stability of substitutional Na<sup>+</sup> and K<sup>+</sup> defects.

## 2. Computational Method

The projector augmented wave (PAW) method, implemented in VASP,<sup>15–17</sup> is used to calculate electronic and atomic structures of substitutional Na<sup>+</sup> and K<sup>+</sup> in HAp. The generalized gradient approximation (GGA) in the functional form by Perdew, Bruke and Ernzerhof is used for the exchange-correlation potential.<sup>18</sup> Electronic wave functions are expanded by plane waves up to a cutoff energy of 500 eV, and all atoms in unit cell and supercells are allowed to relax until the atomic forces converge to less than 0.5 eV/nm.

Figure 1 shows the hexagonal unit cell of HAp (space group *P*6<sub>3</sub>/*m*) viewed along the *c* axis.<sup>19,20</sup> In this structure having total 44 atoms, each P atom is coordinated by four oxygen atoms, forming PO<sub>4</sub> tetrahedra with a P-O bond length of about 0.16 nm, OH groups are arranged along the *c* axis, and there are two different Ca sites (Ca-1 and Ca-2). Ca-1 is surrounded by six PO<sub>4</sub> tetrahedra, and then its coordination number with the first nearest neighboring (NN) oxygen atoms at vertices of the PO<sub>4</sub> tetrahedra and that with the second NN ones are six and three, respectively. In the case of Ca-2, the first NN coordination number with oxygen is six, and one more oxygen atom is situated at the second NN site. However, it is noted here that an OH group arranging along the *c* axis is located at the first NN site of Ca-2.

For defect calculations, 352-atom supercells are generated by doubling the HAp unit cell in three dimensions. One of Ca<sup>2+</sup> ions in the supercell is replaced by Na<sup>+</sup> and K<sup>+</sup>, and the supercell total energy is calculated with structural optimization of all atoms in the supercell. In the supercell calculations, only the  $\Gamma$  point is used for Brillouin-zone sampling.

Based on total energies  $E_T$  of the perfect and defective 352-atom supercells, formation energies ( $\Delta H_f$ ) of substitu-

\*Graduate Student, Kyoto University

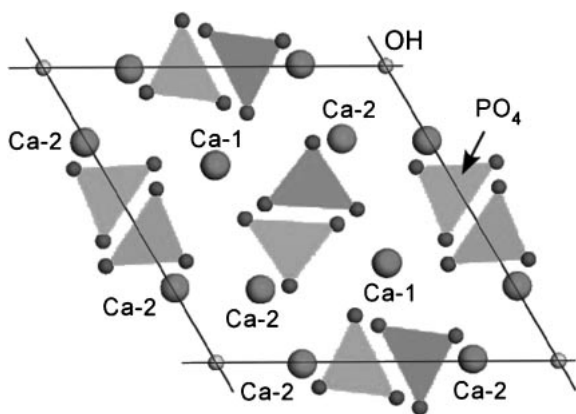


Fig. 1 Crystal structures of hexagonal HAp viewed along the *c* axis. The  $\text{PO}_4^{3-}$  groups are represented by the tetrahedra.

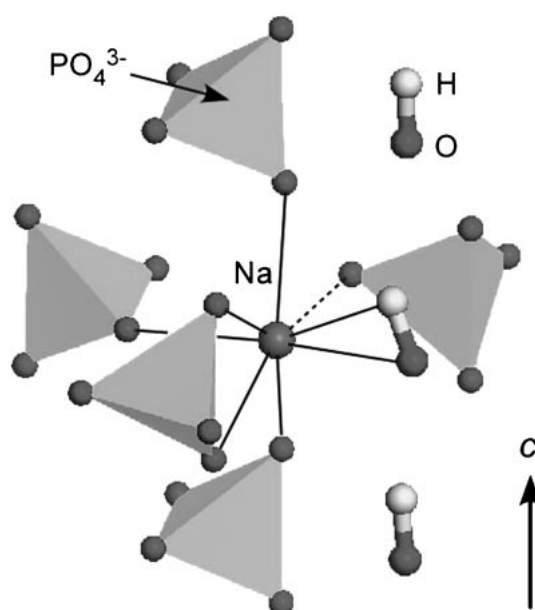


Fig. 2 Optimized atomic structure of substitutional  $\text{Na}^+$  at Ca-2. In order to show the atomic coordination clearly, the first NN atoms are connected to the defect by the solid lines, while the second NN oxygen atom by the broken line.

tional  $\text{Na}^+$  and  $\text{K}^+$  in HAp are evaluated. Detailed description of the formula for  $\Delta H_f$  is also given elsewhere,<sup>12-14</sup> and thus a number of important issues are briefly described. When an ionic species *i* with an ionic charge  $z_i$  is removed ( $l_i = 1$ ) or added ( $l_i = -1$ ) to form a defect with an effective charge  $q$  in HAp, its formation energy can be generally written as

$$\Delta H_f = E_T(\text{defect}; q) - E_T(\text{perfect}) + \sum_i l_i \mu_i. \quad (1)$$

Here  $\mu_i$  indicates a chemical potential for the ionic species *i*.

In this study, the chemical potential  $\mu_i$  is determined by assuming chemical equilibrium between HAp and the aqueous solution saturated with respect to HAp. Hence, the following equation of electrochemical potentials for the ionic species *i* in the solid HAp and the aqueous solution phases ( $\bar{\mu}_{i,\text{HAp}}$  and  $\bar{\mu}_{i,\text{aq}}$ ) is satisfied,

$$\bar{\mu}_{i,\text{HAp}} = \bar{\mu}_{i,\text{aq}}. \quad (2)$$

In terms of inner potentials for HAp and the saturated aqueous solution ( $\phi^{(\text{HAp})}$  and  $\phi^{(\text{aq})}$ ), the chemical potential  $\mu_i$  is given by

$$\mu_{i,\text{HAp}} = \mu_{i,\text{aq}} + z_i(\phi^{(\text{aq})} - \phi^{(\text{HAp})}) = \mu_{i,\text{aq}} + z_i \Delta_{\text{HAp}}^{\text{aq}} \phi. \quad (3)$$

Substituting eq. (3) into (1) gives the following equation,

$$\Delta H_f = E_T(\text{defect}; q) - E_T(\text{perfect}) + \sum_i l_i \mu_{i,\text{aq}} - q \Delta_{\text{HAp}}^{\text{aq}} \phi. \quad (4)$$

Here the following relation between the ionic charge  $z_i$  and the effective charge of the defect  $q$  is used,<sup>12)</sup>

$$q = - \sum_i l_i z_i. \quad (5)$$

The inner potential difference of the last term in the right-hand side of in eq. (4) cannot be calculated theoretically. However, this electrostatic term should be cancelled out due to the charge neutrality requirement in HAp. In the present case, in order to evaluate the thermodynamic stability of  $\text{Na}^+$  and  $\text{K}^+$  ions substituting for  $\text{Ca}^{2+}$  in HAp (these are denoted as  $\text{Na}'_{\text{Ca}}$  and  $\text{K}'_{\text{Ca}}$  according to the Kröger-Vink notation), interstitial protons ( $\text{H}_i^\bullet$ ) and  $\text{OH}^-$  vacancies ( $\text{V}_{\text{OH}}^\bullet$ ) are considered as the charge compensating defects. In practice, therefore, defect formation reactions of  $\text{Na}'_{\text{Ca}} + \text{H}_i^\bullet$ ,  $\text{Na}'_{\text{Ca}} + \text{V}_{\text{OH}}^\bullet$ ,  $\text{K}'_{\text{Ca}} + \text{H}_i^\bullet$ , and  $\text{K}'_{\text{Ca}} + \text{V}_{\text{OH}}^\bullet$  are explicitly investigated.

Finally, the chemical potential for the ionic species *i* in aqueous solution  $\mu_{i,\text{aq}}$  is expressed as

$$\mu_{i,\text{aq}} = \mu_{i,\text{aq}}^\circ + k_B T \ln a_i. \quad (6)$$

$\mu_{i,\text{aq}}^\circ$  means a standard chemical potential,  $k_B$  is the Boltzmann constant,  $T$  is a temperature ( $T = 298$  K throughout this study), and  $a_i$  is an activity. The detailed procedure to evaluate the quantity of  $\mu_{i,\text{aq}}^\circ$  was described elsewhere in detail, where experimental thermodynamic data (e.g., the standard Gibbs formation energy for *i* in aqueous solution) were used.<sup>12-14,21)</sup>

On the other hand, for the activity  $a_i$ , activity coefficients are approximated to be 1.0 throughout the present study, because HAp is sparingly soluble in water and thus the saturated solution is considered as a dilute solution. In addition, it is assumed that the saturated solution contains  $\text{Na}^+$  or  $\text{K}^+$  ions at a given concentration ( $= 1.0 \times 10^{-3}$  mol/L, in this study). Ionic concentrations in the HAp-saturated solution containing  $\text{Na}^+$  or  $\text{K}^+$  are obtained in the manner described in Refs. 13) and 14), where experimental data of the solubility product for HAp, the ionic product of water, three kinds of acid dissociation constants for phosphate ions ( $\text{HPO}_4^{2-} = \text{PO}_4^{3-} + \text{H}^+$ ,  $\text{H}_2\text{PO}_4^- = \text{HPO}_4^{2-} + \text{H}^+$ , and  $\text{H}_3\text{PO}_4 = \text{H}_2\text{PO}_4^- + \text{H}^+$ ), and charge neutrality requirement in the solution are used. Since ionic concentrations in the saturated solution depend on solution pH,<sup>12,22)</sup> chemical potentials for the ionic species also exhibit pH dependence.

As described above, the present study attempts to evaluate formation energies of substitutional  $\text{Na}^+$  and  $\text{K}^+$  in HAp, under chemical equilibrium between HAp and the saturated aqueous solution. In such a case, since the situation that HAp crystals are surrounded by the aqueous solution is assumed, a solvent effect could be important in total energy calculations for HAp supercells,<sup>23)</sup> which, however, is not taken into

account explicitly and is also beyond the scope of this study. Instead, it is simply considered here that the substitutional defects and other charge-compensating defects are formed at atomic sites in bulk HAp far away from the surface, by ion exchange with ions dissolving in aqueous solution.

### 3. Results and Discussion

#### 3.1 Atomic structures around the substitutional defects

When substitutional  $\text{Na}^+$  and  $\text{K}^+$  defects are introduced in HAp, the surrounding ions or ion groups may undergo structural relaxation due to differences of the ionic radii and ionic charges from those of  $\text{Ca}^{2+}$ . In order to investigate detailed atomic coordinations of the defects, interatomic distances from the defects to the surrounding ions and their coordination numbers are listed in Table 1.

For substitutional  $\text{Na}^+$  at the Ca-1 site, the relaxed atomic structure is also displayed in Fig. 2. In this case, it is found from Table 1 that the first NN oxygen atoms move outward from the defect by about 2.5%. This can be understood from the slightly larger ionic radius of  $\text{Na}^+$  (0.102 nm) than that of  $\text{Ca}^{2+}$  (0.100 nm).<sup>6)</sup> In addition,  $\text{Na}^+$  substituting for  $\text{Ca}^{2+}$  has a negative effective charge of  $-1$  ( $\text{Na}'_{\text{Ca}}$ ), and thus the negatively charged oxygen ions at the first NN sites tend to exhibit outward relaxation due to the electrostatic repulsion with the  $\text{Na}^+$  defect. This tendency is applicable to the case of the ionic substitution at Ca-2. Although the interatomic distances from  $\text{Ca}^{2+}$  or  $\text{Na}^+$  at the Ca-2 site to the first NN oxygen atoms range from 0.235 nm to 0.257 nm, the average distance for substitutional  $\text{Na}^+$  at Ca-2 (0.247 nm) is by 2.5% larger than that for  $\text{Ca}^{2+}$  at Ca-2 of the perfect HAp lattice (0.241 nm). It is also noted that, in formation of substitutional  $\text{Na}^+$  at Ca-2, a hydrogen atom is present as the first NN from the defect (at 0.243 nm in distance). The hydrogen atom originally belongs to the OH group located at the first NN site from the Ca-2 site, and yet displaces inwardly due to electrostatic attraction between the positively charged hydrogen atom and the negatively charged substitutional  $\text{Na}^+$ . In practice, such an inward relaxation of the hydrogen atom is realized by rotation of the OH group, as can be seen in Fig. 2.

In the similar way to the  $\text{Na}^+$  substitutions, the substitution of  $\text{K}^+$  induces outward relaxations of the surrounding oxygen atoms. Since  $\text{K}^+$  has a much larger ionic radius (0.138 nm) than  $\text{Ca}^{2+}$  and  $\text{Na}^+$ ,<sup>6)</sup> however, the magnitude of the outward

relaxations of about 9% is larger, as compared to the  $\text{Na}^+$ -substitution cases.

#### 3.2 Formation energies

Based on total energies of the defective supercells, formation energies of substitutional  $\text{Na}^+$  and  $\text{K}^+$  are evaluated. It is noted that the defects have a negative effective charge of  $-1$  because  $\text{Na}^+$  and  $\text{K}^+$  replace  $\text{Ca}^{2+}$  ( $\text{Na}'_{\text{Ca}}$  and  $\text{K}'_{\text{Ca}}$ ), and thus additional charge-compensating defects need to be formed so as to keep charge neutrality of the system. As stated before, therefore, an interstitial proton ( $\text{H}_i^\bullet$ ) and an  $\text{OH}^-$  vacancy ( $\text{V}_{\text{OH}}^\bullet$ ) are considered as the charge compensating defects.

In our previous paper,<sup>12)</sup> the  $\text{H}_i^\bullet$  and  $\text{V}_{\text{OH}}^\bullet$  defects were already calculated in the same manner with the present supercell calculations, and the total energies then obtained are used to evaluate the defect reaction energies for  $\text{Na}'_{\text{Ca}}$  and  $\text{K}'_{\text{Ca}}$ . It is worth mentioning here that a number of interstitial sites for  $\text{H}_i^\bullet$  in HAp were investigated but the interstitial site attached to the  $\text{OH}^-$  group was found to be most stable for the proton,<sup>12)</sup> whose result is used in the present study. It is also noted that no interactions of  $\text{Na}'_{\text{Ca}}$  and  $\text{K}'_{\text{Ca}}$  with the charge compensating defects are explicitly taken into account at the moment. Effects of the defect association will be described later.

Figure 3 indicates calculated formation energies of  $\text{Na}'_{\text{Ca}}$  and  $\text{K}'_{\text{Ca}}$  as a function of solution pH. In order to obtain the formation energies,  $\text{Na}^+$  and  $\text{K}^+$  concentrations ( $[\text{Na}^+]$ ,  $[\text{K}^+]$ ) in the aqueous solution saturated with respect to HAp are assumed to be  $1.0 \times 10^{-3}$  mol/L. Although real body fluids and serum contain different amounts of  $\text{Na}^+$  ( $\sim 10^{-1}$  mol/L) and  $\text{K}^+$  ( $\sim 10^{-3}$  mol/L) ions,<sup>24)</sup> the same value for  $[\text{Na}^+]$  and  $[\text{K}^+]$  is employed here to make direct comparison of the defect formation energies. It can be seen that, in the respective cases of  $\text{Na}'_{\text{Ca}}$  and  $\text{K}'_{\text{Ca}}$ , the defect-formation energies with charge compensating  $\text{H}_i^\bullet$  are smaller, as compared to those with  $\text{V}_{\text{OH}}^\bullet$ . This is because, in HAp, formation of  $\text{H}_i^\bullet$  is more stable than that of  $\text{V}_{\text{OH}}^\bullet$  over the entire pH range, which was found in Ref. 12). Regarding the site preference of the substitutional defects, it is found that both  $\text{Na}'_{\text{Ca}}$  and  $\text{K}'_{\text{Ca}}$  favor substitutions at the Ca-1 site than those at the Ca-2 site.

In addition, Fig. 3 shows that  $\text{Na}'_{\text{Ca}}$  formation is energetically more favorable (by about 0.3 eV per defect) than  $\text{K}'_{\text{Ca}}$ . This can be imagined from the fact that the larger-sized  $\text{K}^+$  substitution than the  $\text{Na}^+$  case induces larger atomic relaxations of the surrounding atoms (see Table 1), which results in the more elastic-energy expense by the substitution. Since the ionic size effect on the defect formation energies of substitutional divalent cations in HAp was previously investigated,<sup>14)</sup> the formation energies of  $\text{Na}'_{\text{Ca}}$  and  $\text{K}'_{\text{Ca}}$  at solution pH = 7 are plotted against the ionic radii in Fig. 4, together with the results for substitutional divalent cations.<sup>14)</sup> It is noted that the ionic concentration  $[\text{M}^{2+}]$  is also set to  $1.0 \times 10^{-3}$  mol/L to evaluate formation energies of the substitutional divalent cations. In this case, the formation energies of  $\text{Na}'_{\text{Ca}}$  and  $\text{K}'_{\text{Ca}}$  at Ca-1 with charge compensating  $\text{H}_i^\bullet$ , which are lowest defect formation energies in Fig. 3, are used. As stated in Ref. 14), the  $\text{Pb}^{2+}$  substitution energy considerably deviates from the ionic-size dependence,

Table 1 Calculated interatomic distances and coordination numbers from isolated substitutional  $\text{Na}^+$  or  $\text{K}^+$  to the nearest neighboring atoms.

Ca site	Distances in nm (Atomic species; Coordination number)		
	First NN	Second NN	
$\text{Ca}^{2+}$	Ca-1	0.244(O;3), 0.248(O;3)	0.280(O;3)
	Ca-2	0.236~0.252(O;6)	0.269(H;1), 0.281(O;1)
$\text{Na}^+$	Ca-1	0.250(O;3), 0.255(O;3)	0.292(O;3)
	Ca-2	0.235~0.257(O;6), 0.243(H;1)	0.298(O;1)
$\text{K}^+$	Ca-1	0.265(O;3), 0.270(O;3)	0.287(O;3)
	Ca-2	0.250~0.275(O;6), 0.263(H;1)	0.291(O;1)

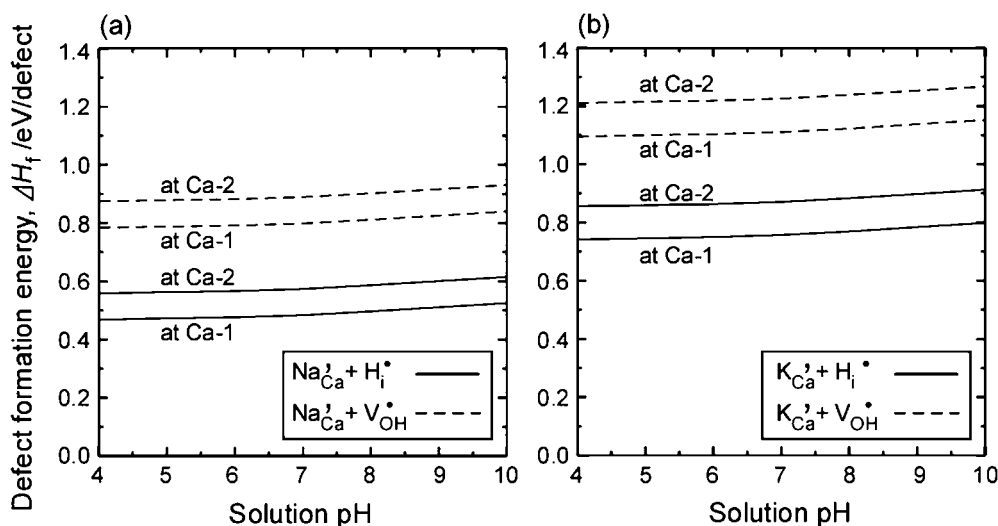


Fig. 3 Defect formation energies of (a)  $\text{Na}'_{\text{Ca}}$  and (b)  $\text{K}'_{\text{Ca}}$  against solution pH. Here the  $\text{Na}^+$  or  $\text{K}^+$  concentration in solution, which is necessary for the substitution energy calculations, is set to be  $1.0 \times 10^{-3}$  mol/L, respectively.

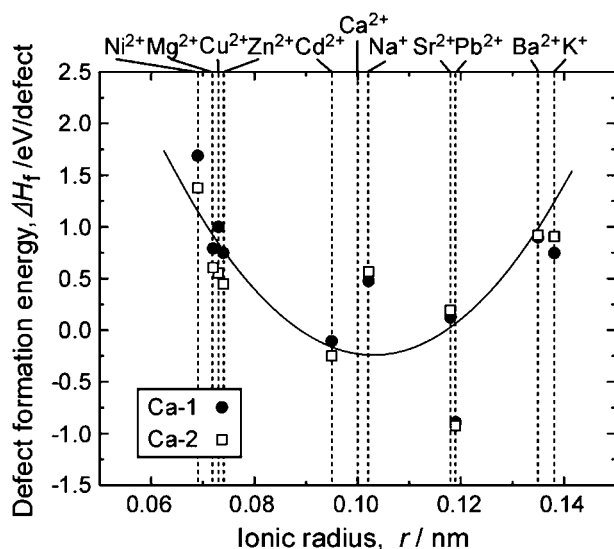


Fig. 4 Defect formation energies per defect species as a function of experimental ionic radii in the sixfold coordination.<sup>6)</sup> In this figure, the formation energies at pH = 7 are used, where the concentrations of the doping species in the aqueous solution are set to  $1.0 \times 10^{-3}$  mol/L. The quadratic curve is obtained by least-square fitting of the data except for  $\text{Pb}^{2+}$ ,  $\text{Na}^+$  and  $\text{K}^+$ .

because its covalent bond formation with the surrounding oxygen atoms. In other words, the chemical bonding state of HAp can be described by an ionic character of bonding and thus the ionic-size mismatches between  $\text{Ca}^{2+}$  and  $\text{M}^{2+}$  generally determine the defect formation energies.

From Fig. 4, it seems that the formation energies of  $\text{Na}'_{\text{Ca}}$  and  $\text{K}'_{\text{Ca}}$  do not scale with the ionic-size differences from  $\text{Ca}^{2+}$ , as found for the substitutional divalent cations. This may be due to the negative effective charge of the defects. In the case of the divalent cations, the effective charges of the defects substituting for  $\text{Ca}^{2+}$  are formally zero, so that it can be expected that the stability of the substitutional defects generally depends on the ionic size mismatch between  $\text{Ca}^{2+}$  and  $\text{M}^{2+}$ . The ionic-size effect could be partly true for the monovalent cations. However, the negative charges of  $\text{Na}'_{\text{Ca}}$

Table 2 Calculated formation energies of the associated defects at pH = 7 and the association energies. The latter quantities are obtained from differences between formation energies of the isolated defect species and those of the associated defects. In this case, the positive values indicate attractive interactions between defect species in the associated pairs.

Defect pair	Formation energy (eV/defect)	Association energy (eV)
$\text{Na}'_{\text{Ca-2}} + \text{H}_i^{\bullet}$	0.21	0.37
$\text{Na}'_{\text{Ca-2}} + \text{V}_{\text{OH}}^{\bullet}$	0.62	0.26
$\text{K}'_{\text{Ca-2}} + \text{H}_i^{\bullet}$	0.70	0.21
$\text{K}'_{\text{Ca-2}} + \text{V}_{\text{OH}}^{\bullet}$	0.92	0.30

and  $\text{K}'_{\text{Ca}}$  undergo electrostatic repulsion with the surrounding oxygen atoms in HAp, and thus the additional electrostatic energy expenses will significantly affect the stability of  $\text{Na}'_{\text{Ca}}$  and  $\text{K}'_{\text{Ca}}$ .

Since the charged defect species in HAp may interact with each other due to electrostatic attraction, effects of defect association on the formation energies  $\text{Na}'_{\text{Ca}}$  and  $\text{K}'_{\text{Ca}}$  are finally investigated. It is noted that  $\text{H}_i^{\bullet}$  in this case is bonded to an  $\text{OH}^-$  group arranging along the  $c$  axis of HAp.  $\text{V}_{\text{OH}}^{\bullet}$  is also located along the  $c$  axis, and thus formation of the associated defects is spatially possible when  $\text{Na}^+$  and  $\text{K}^+$  substitute for Ca-2 (see the crystal structure shown in Fig. 1). In order to evaluate the formation energies of the associated defects, the defect pairs of  $\text{Na}'_{\text{Ca-2}} + \text{H}_i^{\bullet}$ ,  $\text{Na}'_{\text{Ca-2}} + \text{V}_{\text{OH}}^{\bullet}$ ,  $\text{K}'_{\text{Ca-2}} + \text{H}_i^{\bullet}$ , and  $\text{K}'_{\text{Ca-2}} + \text{V}_{\text{OH}}^{\bullet}$  in the nearest neighboring configurations are introduced in the 352-atom supercell, and the relaxed atomic structures and total energies are calculated.

Table 2 lists calculated formation energies of the associated pairs at pH = 7. From the energy differences from the results in Fig. 3, association energies between the defect species in the associated pairs can be obtained, which are also shown in the table. It can be seen that the defect association can decrease the formation energies by about 0.3 eV/defect. As an example, the relaxed atomic structure of the associated  $\text{Na}'_{\text{Ca-2}} + \text{H}_i^{\bullet}$  is displayed in Fig. 5. In this structure,  $\text{Na}'_{\text{Ca-2}}$  is coordinated by three oxygen atoms and one hydrogen atom

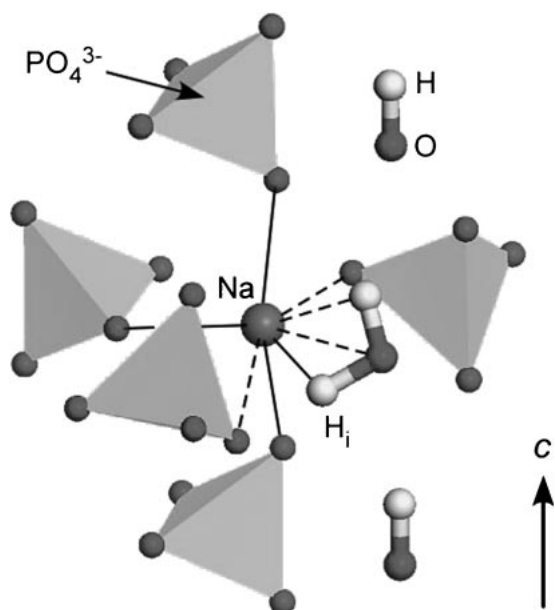


Fig. 5 Optimized atomic structure of the associated pair of  $\text{Na}'_{\text{Ca-2}} + \text{H}_i^{\bullet}$ . In order to show the atomic coordination clearly, the first NN atoms are connected to the defect by the solid lines, while the second NN atoms by the broken lines.

at an average distance of 0.229 nm, while further three oxygen atoms and one hydrogen atom of the  $\text{OH}^-$  group are located at 0.266 nm on average from  $\text{Na}'_{\text{Ca-2}}$ . As also stated in Fig. 2, the  $\text{OH}^-$  group adjacent to  $\text{Na}'_{\text{Ca-2}}$  is rotated off the  $c$  axis so as to orient the positively charged hydrogen atom toward the negatively charged  $\text{Na}'_{\text{Ca-2}}$ . Moreover, the  $\text{H}_i^{\bullet}$  defect is still attached to the  $\text{OH}^-$  group to form the  $\text{H}_2\text{O}$  group. It should be noted that the  $\text{H}_i^{\bullet}$  is located between oxygen atoms of the  $\text{OH}^-$  group and the adjacent  $\text{PO}_4^{3-}$  group. It can be thought, therefore, that the interstitial proton is stabilized by forming the hydrogen-bonding network between  $\text{OH}^-$  and  $\text{PO}_4^{3-}$ .

Especially, the association effect is significant for the associated pair of  $\text{Na}'_{\text{Ca-2}} + \text{H}_i^{\bullet}$ , and its formation energy of 0.21 eV becomes considerably smaller than the lowest defect reaction energy of  $\text{Na}'_{\text{Ca-1}}$  and charge-compensating  $\text{H}_i^{\bullet}$  without association (0.48 eV at pH = 7) shown in Fig. 3. In contrast, the associated pair of  $\text{K}'_{\text{Ca-2}} + \text{H}_i^{\bullet}$  also exhibits the relatively small formation energy of 0.70 eV, as compared to the value of the  $\text{K}'_{\text{Ca-1}}$  and  $\text{H}_i^{\bullet}$  pair without association (0.75 eV at pH = 7). However, the formation energy of the associated  $\text{K}'_{\text{Ca-2}} + \text{H}_i^{\bullet}$  is still much larger than that of the  $\text{Na}'_{\text{Ca-2}} + \text{H}_i^{\bullet}$ .

Based on the above results, it can be said that  $\text{Na}^+$  substitution in HAp is energetically more favorable than  $\text{K}^+$  substitution. This result is at least in qualitative agreement with the fact that the  $\text{Na}^+$  content in bones and tooth enamels (0.5–1.0 mass%) is generally larger than the  $\text{K}^+$  content (0.03–0.10 mass%).<sup>1,2)</sup> Also, it is found that charge compensation and association with interstitial protons play an important role for  $\text{Na}^+$  and  $\text{K}^+$  incorporation into HAp. In order to predict concentrations of substitutional  $\text{Na}^+$  and  $\text{K}^+$  in biological HAp in more detail, however, it is expected that the presence of  $\text{CO}_3^{2-}$  ions should be taken into account. It is known that  $\text{CO}_3^{2-}$  is a most abundant trace element in

biological HAp (about 4–8 mass%) and substitutes for  $\text{OH}^-$  or  $\text{PO}_4^{3-}$ , which may act as a charge compensating defect for other trace elements involved in biological HAp.<sup>1,2)</sup>

#### 4. Summary and Conclusions

First-principles calculations of  $\text{Na}^+$  and  $\text{K}^+$  ions substituting for  $\text{Ca}^{2+}$  in HAp were performed to investigate the atomic structures and the defect formation energies. Since the substitutional defects have a negative effective charge of  $-1$ , formation of additional charge compensating defects is required for the defect formation. In this regard, it is found that interstitial protons can be introduced from the surrounding aqueous solution and act as the charge compensating defect. From the comparison between  $\text{Na}^+$  and  $\text{K}^+$ , substitutional  $\text{Na}^+$  is more stably formed, which may be partly related to the fact that  $\text{Na}^+$  is generally more abundantly involved in bones and tooth enamels than  $\text{K}^+$ .

#### Acknowledgments

This study was supported by Grant-in-Aid for Scientific Research on Priority Areas “Nano Materials Science for Atomic Scale Modification 474” from Ministry of Education, Culture, Sports, Science and Technology (MEXT) of Japan. The authors also acknowledge I. Tanaka for his support of computation.

#### REFERENCES

- 1) S. V. Dorozhkin: *J. Mater. Sci.* **42** (2007) 1061–1095.
- 2) J. C. Elliot: *Reviews in Mineralogy and Geochemistry*, vol. 48, (Mineralogical Society of America, Washington, D.C., USA, 2002) pp. 427–453.
- 3) C. H. Suelter: *Science* **168** (1970) 789–795.
- 4) F. Ginty, A. Flynn and K. D. Cashman: *Br. J. Nutr.* **79** (1998) 343–350.
- 5) H. P. Weismann, U. Plate, K. Zierold and H. J. Höhling: *J. Dent. Res.* **77** (1998) 1654–1657.
- 6) R. A. Shannon: *Acta Cryst. A* **32** (1976) 751–767.
- 7) L. Calderín, M. J. Stott and A. Rubio: *Phys. Rev. B* **67** (2003) 134106.
- 8) P. Rulis, L. Ouyang and W. Y. Ching: *Phys. Rev. B* **70** (2004) 155104.
- 9) J. Terra, M. Jiang and D. E. Ellis: *Philos. Mag. A* **82** (2003) 2357–2377.
- 10) K. Matsunaga and A. Kuwabara: *Phys. Rev. B* **75** (2007) 014102.
- 11) M. Corno, R. Orlando, B. Civalleri and P. Ugliengo: *Eur. J. Mineral.* **19** (2007) 757–767.
- 12) K. Matsunaga: *Phys. Rev. B* **77** (2008) 104106.
- 13) K. Matsunaga: *J. Chem. Phys.* **128** (2008) 245101.
- 14) K. Matsunaga, H. Inamori and H. Murata: *Phys. Rev. B* **78** (2008) 094101.
- 15) G. Kresse and J. Furthmüller: *Phys. Rev. B* **54** (1996) 11169–11186.
- 16) P. E. Blöchl: *Phys. Rev. B* **50** (1994) 17953–17979.
- 17) G. Kresse and D. Joubert: *Phys. Rev. B* **59** (1999) 1758–1775.
- 18) J. P. Perdew, K. Burke and M. Ernzerhof: *Phys. Rev. Lett.* **77** (1996) 3865–3868.
- 19) M. I. Kay, R. A. Young and S. Posner: *Nature* **204** (1964) 1050–1052.
- 20) J. C. Elliot: *Structure and chemistry of the apatites and other calcium orthophosphates*, (Elsevier, Amsterdam, 1994).
- 21) D. D. Wagman, W. H. Evans, V. B. Parker, R. H. Schumm, I. Halow, S. M. Bailey, K. L. Churney and R. L. Nuttall: *J. Phys. Chem. Ref. Data* **11** (1982) 1.
- 22) S. Chandler and D. W. Fuerstenau: *J. Colloid Interface Sci.* **70** (1979) 506–516.
- 23) M. Otani and O. Sugino: *Phys. Rev. B* **73** (2006) 115407.
- 24) T. Kokubo, H. Kushitani, S. Sakka, T. Kitsugi and T. Yamamoto: *J. Biomed. Mater. Res.* **24** (1990) 721–734.